Nonlinear Control of Multi-Rotor Aerial Vehicles Based on the Zero-Moment Direction

Giulia Michieletto * Angelo Cenedese * Luca Zaccarian **,***
Antonio Franchi **

* Dep. of Information Engineering, University of Padova, Padova, Italy
(e-mail: giulia.michieletto@unipd.it, angelo.cenedese@unipd.it)
** LAAS-CNRS, Université de Toulouse, CNRS, Toulouse, France
(e-mail: luca.zaccarian@laas.fr, antonio.franchi@laas.fr)
*** Dep. of Industrial Engineering, University of Trento, Trento, Italy

Abstract:
A quaternion-based nonlinear control strategy is here presented to steer and keep a generic multi-rotor platform in a given reference position. Exploiting a state feedback structure, the proposed solution ensures the stabilization of the aerial vehicle so that its linear and angular velocity are zero and its attitude is constant. The main feature of the designed controller is the identification of a *zero-moment direction* in the feasible force space, i.e., a direction along which the control force intensity can be assigned independently of the control moment. The asymptotic convergence of the error dynamics is confirmed by simulation results on a hexarotor with tilted propellers.

Keywords: UAVs, nonlinear feedback control, hovering.

1. INTRODUCTION

In the last decades, Unmanned Aerial Vehicles (UAVs) have gained a lot of popularity because of their high maneuverability and autonomy, becoming a mature technology exploited in the civil, academic and military context (see Mahony et al. (2012) and references therein). Nowadays such aerial platforms are employed in several application fields ranging from the classical visual sensing tasks to the modern physical interaction.

In this framework, *hovering and trajectory tracking* constitute classical control issues. Hence, in the literature many control strategies are known to enhance the stability properties of a UAV tracking a desired trajectory. They are generally based on linear control systems such as proportional-derivative controllers or linear quadratic regulators, see e.g., (Argentim et al., 2013; Erginer and Altug, 2007). Nonlinear controllers are less popular and mainly exploit feedback linearization (Mistler et al., 2001), sliding mode and backstepping (Bouabdallah and Siegwart, 2005) and geometric control (Lee et al., 2009)).

The effectiveness of such non-linear techniques is confirmed by the experimental tests. For example, Carrillo et al. (2012) have experimentally evaluated the performance of three controllers based on nested saturations, backstepping and sliding mode with the aim of stabilizing the position of a quadrotor w.r.t. an artificial visual landmark on the ground. Similarly, Choi and Ahn (2015) have validated the possibility for a real quadrotor to stably track a point by using a non-linear control strategy that exploits a backstepping-like feedback linearization method.

A deep analysis on the design of feedback control laws for under-actuated aerial vehicles (VTOLs) has been provided by Hua et al. (2013), In their work the authors have stressed the idea that the nonlinear approach to control problems can always be considered as an extension of locally approximating linear control schemes, so that it is possible to derive provable convergence properties by stating certain suitable assumptions. In this sense, Lee et al. (2010) have proved the convergence of their nonlinear tracking controller through Lyapunov theory, assuming bounded initial errors. In detail, they have developed a quadrotor controller that exploits a geometric approach on the manifold of the Special Euclidean Group SE(3) and they have shown that it induces an almost global exponential convergence of the tracking error to the zero equilibrium.

In this context, the contribution of our work can be summarized in the following main aspects. First, we take into account a more generic class of multi-rotor aerial platforms whose dynamics is more complex than the one of standard collinear-rotor vehicles. Specifically, we consider the case in which the propellers are in any number (larger than four) and their spinning axes are generically oriented (including the non-collinear case). This entails the fact that the direction of the control force is not necessarily identified by the third canonical vector and that the control force and the control moment are not fully decoupled as in the typical frameworks studied so far, see e.g., Lee et al. (2010). For such generic platforms, we propose a nonlinear controller based on the identification of a so-called *zero-moment direction*. This concept has been firstly introduced by Michieletto et al. (2017) and refers to a preferential virtual direction in the force space along which the control moment is zero and the intensity of the force can be freely assigned. The designed controller exploits a sort of dynamic feedback linearization around this preferential direction and its implementation allows to asymptotically stabilize the platform to a given reference position, constraining its

linear and angular velocity to be zero (*static hover condition*). The proposed control strategy is based on some algebraic pre-requisites on the control matrices, and its convergence properties are confirmed by the simulation results. Finally, we use the unit quaternion representation of the attitude, overcoming the singularities that characterize the Euler angles and simplifying the equations w.r.t. to the rotation matrices representation.

The rest of the paper is organized as follows. In Section 2 some basic notions on unit quaternion mathematics are given and in Section 3 the dynamic model of a generic multi-rotor platform is derived taking into account the quaternion representation for its attitude. Then, in Section 4 the main contributions is provided, presenting the nonlinear controller, whose convergence properties are validated by means of numerical simulations in Section 5. Finally, in Section 6 some conclusions are drawn.

2. PRELIMINARIES AND NOTATION

To provide a mathematical background for the following proposed model and controller, this section briefly summarizes the basic properties of unit quaternions (Diebel (2006)).

A quaternion is a hyper-complex number, which is generally represented as a four dimensional vector composed by a scalar part, $\eta \in \mathbb{R}$, and a vector part, $\boldsymbol{\varepsilon} \in \mathbb{R}^3$, namely

$$\mathbf{q} := \begin{bmatrix} \eta \\ \boldsymbol{\varepsilon} \end{bmatrix}. \tag{1}$$

A quaternion is said to be *unit* if it has unitary norm, i.e., $\eta^2 + \|\boldsymbol{\varepsilon}\|^2 = 1$. In this case, it belongs to the unit 4D hypersphere $\mathbb{S}^3$ embedded in $\mathbb{R}^4$.

Each unit quaternion is associated to a unique rotation matrix belonging to the Special Orthogonal group $SO(3) := \{\mathbf{R} \in \mathbb{R}^{3 \times 3} \,|\, \mathbf{R}^\top \mathbf{R} = \mathbf{I}_3, \det(\mathbf{R}) = 1\}$. Specifically, given a unit quaternion $\mathbf{q}$, the corresponding rotation matrix is computed as

$$\mathbf{R}(\mathbf{q}) = \mathbf{I}_3 + 2\eta[\boldsymbol{\varepsilon}]_\times + 2[\boldsymbol{\varepsilon}]_\times^2, \tag{2}$$

where the operator $[\cdot]_\times$ denotes the map that associates any non-zero vector in $\mathbb{R}^3$ to the corresponding skew-symmetric matrix in the special orthogonal Lie algebra $\mathfrak{so}(3)$. It can be verified that $\mathbf{R}(\mathbf{q})^\top \mathbf{R}(\mathbf{q}) = \mathbf{I}_3$ and that $\mathbf{q}_I := [1\ 0\ 0\ 0]^\top$ is an *identity* (unit) quaternion (ensuring $\mathbf{R}(\mathbf{q}_I) = \mathbf{I}_3$). We also recall the useful identity $[\boldsymbol{\varepsilon}_1]_\times[\boldsymbol{\varepsilon}_2]_\times + \boldsymbol{\varepsilon}_1^\top \boldsymbol{\varepsilon}_2 \mathbf{I}_3 - \boldsymbol{\varepsilon}_2 \boldsymbol{\varepsilon}_1^\top = \mathbf{0}$.

The relationship between rotation matrices and unit quaternions is not biunivocal: each rotation matrix corresponds to two unit quaternions. Indeed, it holds that $\mathbf{R}(\mathbf{q}) = \mathbf{R}(-\mathbf{q})$. This fact is justified by considering another representation for a unit quaternion, namely

$$\mathbf{q} = \begin{bmatrix} \cos\left(\frac{\theta}{2}\right) \\ \mathbf{u}\sin\left(\frac{\theta}{2}\right) \end{bmatrix}, \tag{3}$$

where $\mathbf{u} \in \mathbb{S}^2$ denotes the rotation axis and $\theta \in [-\pi, +\pi]$ is the corresponding rotation angle. Note that a rotation by $-\theta$ about $-\mathbf{u}$ is represented by the same unit quaternion associated to a rotation by θ about $\mathbf{u}$ (*double coverage property*).

Multiplication of two quaternions $\mathbf{q}_1, \mathbf{q}_2$ is performed by the *quaternion product*, denoted as $\otimes$, which is defined as follows

$$\mathbf{q}_1 \otimes \mathbf{q}_2 = \mathbf{M}(\mathbf{q}_1)\mathbf{q}_2 = \mathbf{N}(\mathbf{q}_2)\mathbf{q}_1 \tag{4}$$

where

$$\mathbf{M}(\mathbf{q}) := \begin{bmatrix} \eta & -\boldsymbol{\varepsilon}^\top \\ \boldsymbol{\varepsilon} & \eta\mathbf{I}_3 + [\boldsymbol{\varepsilon}]_\times \end{bmatrix}, \quad \mathbf{N}(\mathbf{q}) := \begin{bmatrix} \eta & -\boldsymbol{\varepsilon}^\top \\ \boldsymbol{\varepsilon} & \eta\mathbf{I}_3 - [\boldsymbol{\varepsilon}]_\times \end{bmatrix}. \tag{5}$$

Note that using $\mathbf{q}_3 := \mathbf{q}_1 \otimes \mathbf{q}_2$, one has $\mathbf{R}(\mathbf{q}_3) = \mathbf{R}(\mathbf{q}_1)\mathbf{R}(\mathbf{q}_2)$.

Exploiting the quaternion product, it can be verified that the inverse of a given quaternion $\mathbf{q}$ may be chosen as

$$\mathbf{q}^{-1} = \begin{bmatrix} \eta \\ -\boldsymbol{\varepsilon} \end{bmatrix}. \tag{6}$$

Finally, denoting by $\boldsymbol{\omega}$ the angular velocity vector in the body frame of reference, the derivative of a unit quaternion $\mathbf{q}$ is computed as

$$\dot{\mathbf{q}} = \frac{1}{2}\begin{bmatrix} 0 \\ \boldsymbol{\omega} \end{bmatrix} \otimes \mathbf{q} = \frac{1}{2}\mathbf{N}(\mathbf{q})\begin{bmatrix} 0 \\ \boldsymbol{\omega} \end{bmatrix} = \frac{1}{2}\begin{bmatrix} -\boldsymbol{\varepsilon}^\top \\ \eta\mathbf{I}_3 - [\boldsymbol{\varepsilon}]_\times \end{bmatrix}\boldsymbol{\omega}. \tag{7}$$

Conversely, when the angular velocity is expressed in the fixed frame ($\boldsymbol{\omega}' = \mathbf{R}(\mathbf{q})\boldsymbol{\omega}$), the relation (7) is replaced by

$$\dot{\mathbf{q}} = \frac{1}{2}\mathbf{q} \otimes \begin{bmatrix} 0 \\ \boldsymbol{\omega}' \end{bmatrix} = \frac{1}{2}\mathbf{M}(\mathbf{q})\begin{bmatrix} 0 \\ \boldsymbol{\omega}' \end{bmatrix} = \frac{1}{2}\begin{bmatrix} -\boldsymbol{\varepsilon}^\top \\ \eta\mathbf{I}_3 + [\boldsymbol{\varepsilon}]_\times \end{bmatrix}\boldsymbol{\omega}'. \tag{8}$$

3. MULTI-ROTOR VEHICLE DYNAMIC MODEL

This section is devoted to the derivation of the dynamic model of a generic aerial multi-rotor platform, composed by a rigid body and $n \geq 4$ propellers each one spinning about a certain axis. Regarding the rotors, we assume that their mass, gyroscopic effect and moment of inertia w.r.t. the body inertial parameters are all negligible. In addition, their spinning axes could be all parallel oriented or generically tilted. The axes mutual orientation, jointly with the number n of rotors, determines if a given UAV is an under-actuated or a fully-actuated system.

To describe the dynamics of such a multi-rotor vehicle, we introduce $\mathscr{F}_W = \{O_W, (\mathbf{x}_W, \mathbf{y}_W, \mathbf{z}_W)\}$ and $\mathscr{F}_B = \{O_B, (\mathbf{x}_B, \mathbf{y}_B, \mathbf{z}_B)\}$, denoting the inertial *world frame* and the *body frame* attached to the platform, respectively. The origin O_B of $\mathscr{F}_B$ is chosen coincident with the center of mass (CoM) of the vehicle and its position in $\mathscr{F}_W$ is specified by $\mathbf{p} \in \mathbb{R}^3$. The orientation of $\mathscr{F}_B$ w.r.t. $\mathscr{F}_W$ is instead represented by the unit quaternion $\mathbf{q} \in \mathbb{S}^3$. Hence, the pair $(\mathbf{p}, \mathbf{q}) \in \mathbb{R}^3 \times \mathbb{S}^3$ describes the full-pose of the platform in $\mathscr{F}_W$, while its orientation kinematics is governed by (7), where $\boldsymbol{\omega}$ represents the angular velocity of $\mathscr{F}_B$ w.r.t. $\mathscr{F}_W$, expressed in $\mathscr{F}_B$, whereas the linear velocity of O_B in $\mathscr{F}_W$ is referred as $\mathbf{v} = \dot{\mathbf{p}}$.

Let us denote the (controllable) spinning rate of each propeller by ω_i, with $i \in \{1, \dots n\}$. While rotating, each rotor exerts a *thrust force* $\mathbf{f}_i$ and a *drag moment* $\boldsymbol{\tau}_i$, both applied in its CoM and oriented along the direction defined by its spinning axis [1] $\mathbf{z}_{P_i}$. These two quantities are related to the spinning rate by means of a quadratic relation depending on the constant parameters c_{f_i} and c_{τ_i}, respectively. Specifically, the thrust force and the drag moment of the i-th propeller in $\mathscr{F}_B$ result to be

$$\mathbf{f}_i = c_{f_i}\omega_i^2 \mathbf{z}_{P_i} \quad \text{and} \quad \boldsymbol{\tau}_i = \pm\, c_{\tau_i}\omega_i^2 \mathbf{z}_{P_i}, \tag{9}$$

where the presence of a positive (negative) sign in (9) takes into account the clockwise (counterclockwise) rotation direction of the propeller.

The sum of all the propeller thrust forces coincides with the *control force* $\mathbf{f}_c$ applied at the platform CoM. Similarly, the *control moment* $\boldsymbol{\tau}_c$ turns out to be the sum of all the moment contributions due to both the thrust forces and the drag moments. Formally, they can be expressed in the body frame as

---

[1] We assume that the orientation of each $\mathbf{z}_{P_i}$ w.r.t. the platform rotation axis $\mathbf{z}_B$ is constant during the flight, i.e., tiltable platforms are not considered here.
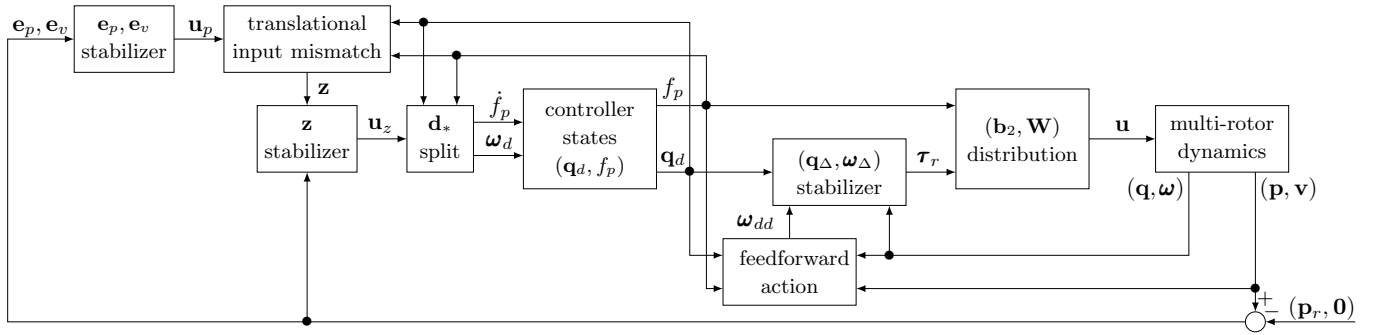
Fig. 1. Block diagram of the closed-loop system with the proposed dynamic control strategy.

$$\mathbf{f}_c = \sum_{i=1}^{n} \mathbf{f}_i \quad \text{and} \quad \boldsymbol{\tau}_c = \sum_{i=1}^{n}((\mathbf{p}_i \times \mathbf{f}_i) + \boldsymbol{\tau}_i), \qquad (10)$$

where $\mathbf{p}_i$ is the position of the CoM of the i-th propeller in $\mathscr{F}_B$.

Using the Newton-Euler approach and neglecting the aforementioned second order effects, the dynamics of the (generic) multi-rotor vehicle is governed by the following system of equations

$$\begin{cases} m\ddot{\mathbf{p}} = -mg\mathbf{e}_3 + \mathbf{R}(\mathbf{q})\mathbf{f}_c & (11) \\ \mathbf{J}\dot{\boldsymbol{\omega}} = -\boldsymbol{\omega} \times \mathbf{J}\boldsymbol{\omega} + \boldsymbol{\tau}_c & (12) \\ \dot{\mathbf{q}} = \dfrac{1}{2} \begin{bmatrix} 0 \\ \boldsymbol{\omega} \end{bmatrix} \otimes \mathbf{q} & (13) \end{cases}$$

where $m > 0$ is the mass of the platform, g is the gravitational constant, and $\mathbf{e}_i$ is the i-th canonical versor in $\mathbb{R}^3$ with $i \in \{1, 2, 3\}$. The positive definite matrix $\mathbf{J} \in \mathbb{R}^{3 \times 3}$ denotes the vehicle inertia matrix w.r.t. O_B expressed in $\mathscr{F}_B$. Note that $\mathbf{R}(\mathbf{q})\mathbf{f}_c$ indicates the control force in $\mathscr{F}_W$.

Exploiting (10), we can rewrite the control force and moment in the motion equations (11)-(12) as

$$\mathbf{f}_c = \mathbf{F}_1 \mathbf{u} \quad \text{and} \quad \boldsymbol{\tau}_c = \mathbf{F}_2 \mathbf{u}, \qquad (14)$$

where $\mathbf{u} = [u_1 \ \ldots \ u_n]^\top = [\omega_1|\omega_1| \ \ldots \ \omega_n|\omega_n|]^\top \in \mathbb{R}^n$ is the *control input vector* and matrices $\mathbf{F}_1, \mathbf{F}_2 \in \mathbb{R}^{3 \times n}$ are the *control matrices* that map $\mathbf{u}$ to the control force and the control moment (expressed in $\mathscr{F}_B$), respectively.

4. ZERO-MOMENT FORCE DIRECTION CONTROLLER

In this section we present the design of a nonlinear control law to stabilize in static hover condition the generic class of multi-rotor platforms described in Section 3.

Problem 1. Given plant (11)–(14), find a (possibly dynamic) state feedback control law assigning input $\mathbf{u}$ in (14), ensuring that for any *constant reference position* $\mathbf{p}_r \in \mathbb{R}^3$, the closed-loop system is able to asymptotically stabilize $\mathbf{p}_r$ with some hovering orientation. In other words, the controller asymptotically stabilizes a set where $\mathbf{p} = \mathbf{p}_r$, and $\dot{\mathbf{p}}$ and $\boldsymbol{\omega}$ are both zero, while orientation $\mathbf{q}$ could be arbitrary but constant.

Note that allowing for an arbitrary orientation is a key towards the feasibility of Problem 1, which is in general solvable only if certain steady-state orientations are reached by the platform. These orientations are strongly connected with the concept of "hoverability". In particular, a solution to Problem 1 does not always exist and its feasibility is related to suitable properties of matrices $\mathbf{F}_1$ and $\mathbf{F}_2$ in (14). Here we make some possibly restrictive assumptions (even though some of them can actually

be proven to be necessary), which are stated in Section 4.1. Then in Section 4.2 we present the dynamics and interconnections of the proposed control scheme (represented in Figure 1). Finally, in Sections 4.3 we derive the error dynamics claiming its asymptotic convergence.

4.1 Assumptions

The stabilizing controller given in this section is based on the following standing assumption.

Assumption 1. The control matrices $\mathbf{F}_1$ and $\mathbf{F}_2$ introduced in (14) satisfy the following properties:

1) $rk(\mathbf{F}_2) = 3$;
2) $\exists \mathbf{b}_2 \in \ker(\mathbf{F}_2) \cap \mathbb{S}^{n-1}$ such that $\mathbf{F}_1 \mathbf{b}_2 \neq \mathbf{0}$;
3) $\exists \mathbf{K} \in \mathbb{R}^{n \times n}$ such that $\mathbf{F}_1 \mathbf{K} \mathbf{F}_2^\top (\mathbf{F}_2 \mathbf{K} \mathbf{F}_2^\top)^{-1} = \mathbf{F}_1 \mathbf{F}_2^{\dagger K} = \mathbf{0}$.

Requirement 1) in Assumption 1 implies the possibility to freely assign the control moment $\boldsymbol{\tau}_c$ in a sufficiently large open space of $\mathbb{R}^3$ containing $\mathbf{0}$ and corresponds to requiring full-actuation of the orientation dynamics (12).

Requirement 2) in Assumption 1 implies the existence of at least a unit vector in $\mathbb{R}^n$ (i.e., a direction in the control input space) that generates a zero control moment and, at the same time, identifies a nonzero control force direction.

Even though this is equivalent to imposing $rk([\mathbf{F}_1^\top \ \mathbf{F}_2^\top]) \geq 4$, the definition of $\mathbf{b}_2$ turns useful to define a key element of our control method, as it will be clear in Section 4.2.

Requirement 3) in Assumption 1, where $\mathbf{F}_2^{\dagger K} \in \mathbb{R}^{n \times 3}$ denotes the *generalized right pseudo-inverse* of $\mathbf{F}_2$, translates into the requirement that the row space of $\mathbf{F}_1$ is orthogonal to the row space of $\mathbf{F}_2$ transformed via matrix $\mathbf{K}$. This constraint essentially enables a sufficient level of decoupling between $\mathbf{f}_c$ and $\boldsymbol{\tau}_c$, and is not too restrictive. For example, let us consider classical multi-rotor systems, which are characterized by parallel propeller directions, balanced geometry of the rotor positions and balanced choice of clockwise/counterclockwise spinning propellers. In this case the condition $\mathbf{F}_1 \mathbf{F}_2^{\dagger K} = \mathbf{0}$ is satisfied by simply choosing $\mathbf{K} = \mathbf{I}_3$ when the number of propellers is even and they are pairwise balanced, i.e., $\mathbf{p}_i + \mathbf{p}_{i+n/2} = \mathbf{0}$, $c_{f_i} = c_{f_{i+n/2}}$, and $\pm c_{\tau_i} = \mp c_{\tau_{i+n/2}}$ for i spanning any number in the range $[1, n/2]$. This configuration is the one considered in Lee et al. (2010), but our Assumption 1 is much weaker, as clearly illustrated by our example study of Section 5.

$$\boldsymbol{\omega}_{dd} := \frac{1}{f_p} \frac{[\mathbf{R}(\mathbf{q}_d)\mathbf{d}_*]_\times}{\|\mathbf{d}_*\|^2} \left(\left(\frac{k_{pd}^2}{m^2} - \frac{k_{pp}}{m} \right) (\mathbf{R}(\mathbf{q})\mathbf{d}_* f_p - k_{pp}\mathbf{e}_p) + \left(2\frac{k_{pp}k_{pd}}{m} - \frac{k_{pd}^3}{m^2} \right) \mathbf{e}_v + \left(\frac{k_{pd}^2}{m^2} - \frac{k_{pp}}{m} - \frac{k_{pd}k_z}{m} + k_z^2 \right) \mathbf{z} \right) \quad (15)$$

4.2 Controller Scheme

The starting point of the proposed controller is based on focusing on what we call the *zero-moment preferential direction* in the force space, denoted by $\mathbf{d}_* \in \mathrm{Im}(\mathbf{F}_1)$. Specifically, vector $\mathbf{d}_*$ identifies a direction along which the intensity $\|\mathbf{f}_c\|$ of the control force can be arbitrarily assigned when the control moment $\boldsymbol{\tau}_c$ is equal to zero. As a consequence, such a direction has to be defined based on the null space of $\mathbf{F}_2$. Recalling Requirement 2) of Assumption 1, a suitable choice is

$$\mathbf{d}_* = \mathbf{F}_1\mathbf{b}_2. \quad (16)$$

Based on the requirements in Assumption 1, we propose here a dynamic controller, where the control input $\mathbf{u}$ is selected as

$$\mathbf{u} = \mathbf{F}_2^{\dagger K}\boldsymbol{\tau}_r + \mathbf{b}_2 f_p, \quad (17)$$

so that vector $\boldsymbol{\tau}_r \in \mathbb{R}^3$ and scalar f_p appear conveniently in dynamics (14) implying

$$\mathbf{f}_c = \mathbf{F}_1\mathbf{u} = \mathbf{d}_* f_p, \quad (18)$$
$$\boldsymbol{\tau}_c = \mathbf{F}_2\mathbf{u} = \boldsymbol{\tau}_r, \quad (19)$$

which clearly reveals a nice decoupling feature behind Assumption 1 and selection (17). Once this decoupling is in place, it is of interest to steer the the platform in a *desired orientation* $\mathbf{q}_d$ such that the direction of the resulting force $\mathbf{R}(\mathbf{q}_d)\mathbf{f}_c$ acting on the translational dynamics (11) (i.e., the direction of $\mathbf{R}(\mathbf{q}_d)\mathbf{d}_*$) coincides with a desired direction arising from a simple PD + gravity compensation feedback function, selected here as

$$\mathbf{u}_p := mg\mathbf{e}_3 - k_{pp}\mathbf{e}_p - k_{pd}\mathbf{e}_v, \quad (20)$$

where $\mathbf{e}_p = \mathbf{p} - \mathbf{p}_r$ and $\mathbf{e}_v = \mathbf{v}$ are the *position error* and the *velocity error*, respectively, while k_{pp} and k_{pd} are arbitrary positive scalar PD gains. Rather than selecting $\mathbf{q}_d$ directly, we prefer here to introduce a state in our controller, evolving in $\mathbb{S}^3$ through the quaternion-based dynamics in (8), namely

$$\dot{\mathbf{q}}_d = \frac{1}{2}\mathbf{q}_d \otimes \begin{bmatrix} 0 \\ \boldsymbol{\omega}_d \end{bmatrix}, \quad (21)$$

where $\boldsymbol{\omega}_d$ is an additional virtual input that should be selected so that the actual input to the translational dynamics (11) eventually converges to the state feedback in (20). In other words, $\boldsymbol{\omega}_d$ should be set in such a way to drive to zero the following mismatch, motivated by (11) and (18),

$$\mathbf{z} := \mathbf{R}(\mathbf{q}_d)\mathbf{f}_c - \mathbf{u}_p = \mathbf{R}(\mathbf{q}_d)\mathbf{d}_* f_p - \mathbf{u}_p. \quad (22)$$

In particular, we will show that such a convergence is ensured by considering the variable f_p in (17) as an additional scalar state of the controller, and then imposing

$$\boldsymbol{\omega}_d = \frac{1}{f_p}[\mathbf{R}(\mathbf{q}_d)\mathbf{d}_*]_\times \mathbf{u}_z, \quad (23)$$

$$\dot{f}_p = (\mathbf{R}(\mathbf{q}_d)\mathbf{d}_*)^\top \mathbf{u}_z, \quad (24)$$

where the first equation clearly makes sense only if $f_p \neq 0$ and where we choose

$$\mathbf{u}_z := \frac{\left(\frac{k_{pd}k_{pp}}{m}\mathbf{e}_p + \left(\frac{k_{pd}^2}{m} - k_{pp} \right)\mathbf{e}_v + \left(\frac{k_{pd}}{m} - k_z \right)\mathbf{z} \right)}{\|\mathbf{d}_*\|^2}, \quad (25)$$

being k_z an additional positive scalar gain.

The scheme is completed by an appropriate selection of $\boldsymbol{\tau}_r$ in (17) ensuring that the actual attitude $\mathbf{q}$ indeed tracks the desired attitude $\mathbf{q}_d$. This task is simple because of Assumption 1, which guarantees the full-authority control action acting on the rotational dynamics, in (19). To simplify the exposition, let us introduce the mismatch $\mathbf{q}_\Delta$ between the current and the desired orientation, namely

$$\mathbf{q}_\Delta = \mathbf{q}_d^{-1} \otimes \mathbf{q} = \begin{bmatrix} \eta_d\eta + \boldsymbol{\varepsilon}_d^\top\boldsymbol{\varepsilon} \\ -\eta\boldsymbol{\varepsilon}_d + \eta_d\boldsymbol{\varepsilon} - [\boldsymbol{\varepsilon}_d]_\times\boldsymbol{\varepsilon} \end{bmatrix} = \begin{bmatrix} \eta_\Delta \\ \boldsymbol{\varepsilon}_\Delta \end{bmatrix}. \quad (26)$$

Then the *reference moment* $\boldsymbol{\tau}_r$ in (17) ensuring the convergence to zero of this mismatch is selected as

$$\boldsymbol{\tau}_r = -k_{ap}\boldsymbol{\varepsilon}_\Delta - k_{ad}(\boldsymbol{\omega} - \mathbf{R}^\top(\mathbf{q})\boldsymbol{\omega}_d) + \boldsymbol{\omega} \times \mathbf{J}\boldsymbol{\omega}$$
$$- \mathbf{J}[\boldsymbol{\omega}]_\times\mathbf{R}^\top(\mathbf{q})\boldsymbol{\omega}_d + \mathbf{J}\mathbf{R}^\top(\mathbf{q})\boldsymbol{\omega}_{dd}, \quad (27)$$

where the PD gains k_{ap} and k_{ad} are any two positive scalars allowing one to tune the proportional and derivative action of the attitude transient, respectively. In equation (27), one clearly sees a feedforward term canceling out the quadratic terms in $\boldsymbol{\omega}$ appearing in (12), in addition to a correction term $\boldsymbol{\omega}_{dd}$ ensuring the forward invariance of the set where $\mathbf{q} = \mathbf{q}_d$ and $\boldsymbol{\omega} = \boldsymbol{\omega}_d$. The expression of this term is reported in equation (15) at the top of the page and can be proved to be equal to $\dot{\boldsymbol{\omega}}_d$ along solutions.

4.3 Error dynamics

To establish useful properties of the closed-loop system presented in the previous section, we first recall the difference $\mathbf{q}_\Delta$ in (26) between the current and the desired orientation. From (26) we have $\mathbf{R}(\mathbf{q}_\Delta) = \mathbf{R}^\top(\mathbf{q}_d)\mathbf{R}(\mathbf{q})$, whose derivative is

$$\dot{\mathbf{R}}(\mathbf{q}_\Delta) = \mathbf{R}^\top(\mathbf{q}_d)\mathbf{R}(\mathbf{q})\left([\boldsymbol{\omega}]_\times - \mathbf{R}^\top(\mathbf{q})[\boldsymbol{\omega}_d]_\times\mathbf{R}(\mathbf{q}) \right) \quad (28)$$

$$= \mathbf{R}(\mathbf{q}_\Delta)\left[\boldsymbol{\omega} - \mathbf{R}^\top(\mathbf{q})\boldsymbol{\omega}_d \right]_\times \quad (29)$$

$$= \mathbf{R}(\mathbf{q}_\Delta)[\boldsymbol{\omega}_\Delta]_\times, \quad (30)$$

where we use $\dot{\mathbf{R}}(\mathbf{q}_d) = [\boldsymbol{\omega}_d]_\times\mathbf{R}(\mathbf{q}_d)$ from (21) and $\dot{\mathbf{R}}(\mathbf{q}) = \mathbf{R}(\mathbf{q})[\boldsymbol{\omega}]_\times$ from (13) (for these relations, see (Diebel, 2006, Eq. 156-157)). Note that we also exploit the following property derived from the rotational invariance of the cross-product: $\mathbf{R}(\mathbf{q})^\top[\boldsymbol{\omega}_d]_\times\mathbf{R}(\mathbf{q}) = \left[\mathbf{R}(\mathbf{q})^\top\boldsymbol{\omega}_d\right]_\times\mathbf{R}(\mathbf{q})^\top\mathbf{R}(\mathbf{q}) = \left[\mathbf{R}(\mathbf{q})^\top\boldsymbol{\omega}_d\right]_\times$.

Relation $\dot{\mathbf{R}}(\mathbf{q}_\Delta) = \mathbf{R}(\mathbf{q}_\Delta)[\boldsymbol{\omega}_\Delta]_\times$ in (30) allows establishing the following relevant dynamics for the *orientation error* variable $\mathbf{q}_\Delta$ and the associated *angular velocity mismatch* $\boldsymbol{\omega}_\Delta$

$$\dot{\mathbf{q}}_\Delta = \frac{1}{2}\begin{bmatrix} 0 \\ \boldsymbol{\omega}_\Delta \end{bmatrix} \otimes \mathbf{q}_\Delta, \quad (31)$$

$$\mathbf{J}\dot{\boldsymbol{\omega}}_\Delta = -\boldsymbol{\omega} \times \mathbf{J}\boldsymbol{\omega} + \mathbf{J}[\boldsymbol{\omega}]_\times\mathbf{R}^\top(\mathbf{q})\boldsymbol{\omega}_d - \mathbf{J}\mathbf{R}^\top(\mathbf{q})\boldsymbol{\omega}_{dd} + \boldsymbol{\tau}_r. \quad (32)$$

where we use $\dot{\mathbf{R}}^\top(\mathbf{q}) = -[\boldsymbol{\omega}]_\times\mathbf{R}^\top(\mathbf{q})$ and where we exploit the identity $\dot{\boldsymbol{\omega}}_d = \boldsymbol{\omega}_{dd}$.

To establish useful properties of the translational dynamics, we evaluate the error vector $\mathbf{e} := [\mathbf{e}_p \ \mathbf{e}_v]^\top$, which well characterizes the deviation from the reference position $\mathbf{p}_r \in \mathbb{R}^3$. Combining the plant equation (11) with the definition of $\mathbf{z}$ given in (22) the dynamics of $\mathbf{e}$ can be rewritten as follows

$$\dot{\mathbf{e}}_p = \mathbf{e}_v \quad (33)$$
$$m\dot{\mathbf{e}}_v = -mg\mathbf{e}_3 + (\mathbf{R}(\mathbf{q}) - \mathbf{R}(\mathbf{q}_d))\mathbf{f}_c + \mathbf{u}_p + \mathbf{z}. \quad (34)$$
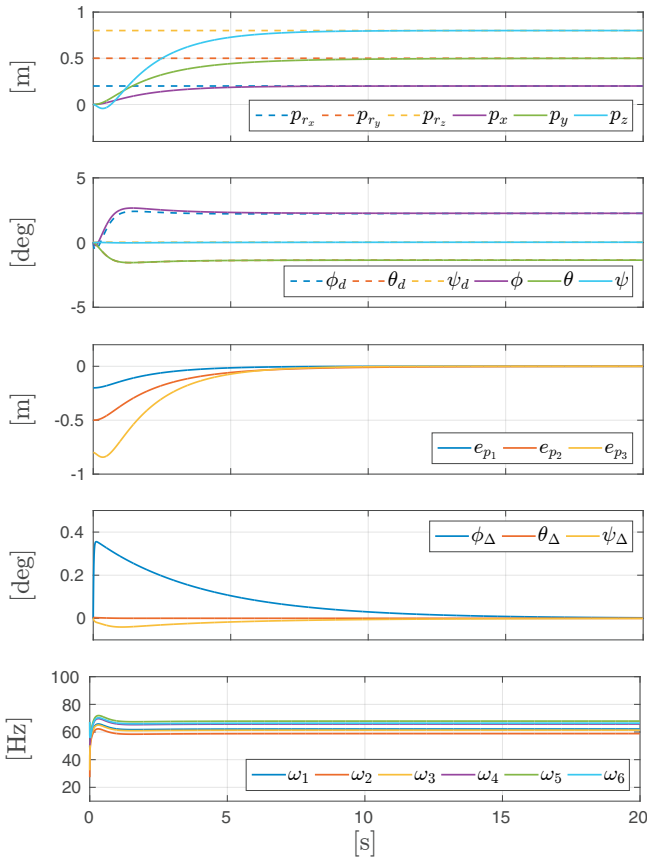
Fig. 2. Static hover control of the hexarotor in ideal conditions: the errors converge to zero and the control inputs belong to a feasible range.
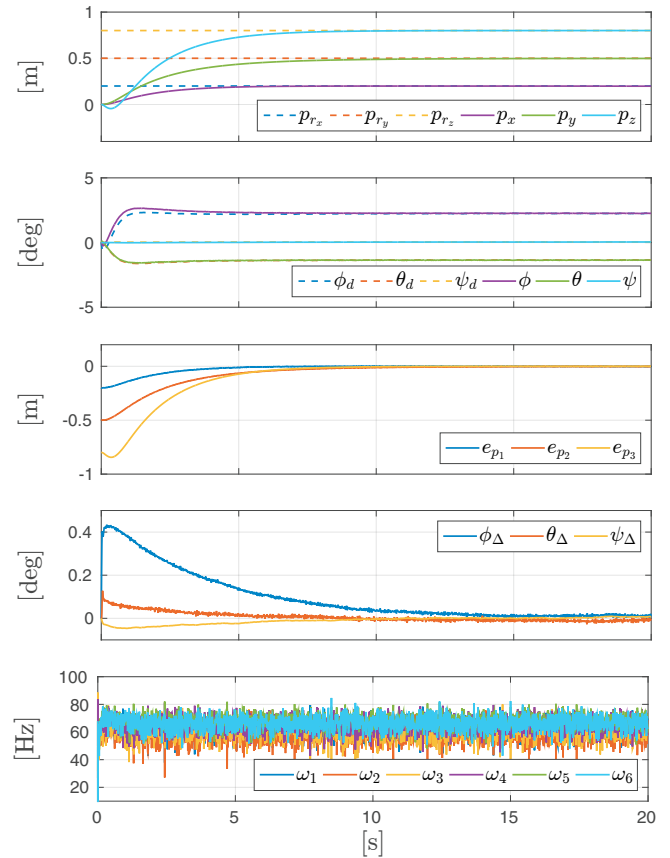

Fig. 3. Static hover control of the hexarotor in real conditions: the controller is robust to the introduction of noise and delays.

A last mismatch variable that needs to be characterized relates to the controller state f_p. In particular, combining (11) with (18), one realizes that the zero position error condition $\mathbf{e}_p = \mathbf{0}$ can only be reached if the state f_p, governed by (24), converges to the value $mg/\|\mathbf{d}_*\|$. Rather than describing the error system in terms of the deviation $f_p - mg/\|\mathbf{d}_*\|$ (which should clearly go to zero), we prefer to use the redundant set of coordinates $\mathbf{z}$ in (22). Indeed, manipulating (22) it is clear that showing that $\mathbf{z}$ tends to zero implies that, asymptotically, we get $\mathbf{R}(\mathbf{q}_d)\mathbf{d}_* f_p = \mathbf{u}_p$. Namely, as long as $\mathbf{e}$ tends to zero too, we approach the set where $\mathbf{d}_* f_p = mg\mathbf{R}^\top(\mathbf{q}_d)\mathbf{e}_3$. Keeping in mind that $\mathbf{q}_\Delta = \mathbf{q}_I$ implies $\mathbf{R}(\mathbf{q}) = \mathbf{R}(\mathbf{q}_d)$, this clearly corresponds to the set characterized in Problem 1 where the orientation satisfies $\mathbf{R}(\mathbf{q})\mathbf{d}_* = \mathbf{R}(\mathbf{q}_d)\mathbf{d}_* = \mathbf{e}_3$ and $\|\mathbf{d}_*\|\|f_p\| = mg$.

To formalize these observation, let us consider the following coordinates for the overall closed loop

$$\boldsymbol{\xi} := (\mathbf{q}_\Delta, \boldsymbol{\omega}_\Delta, \mathbf{z}, \mathbf{e}, \mathbf{q}) \in \Xi, \qquad (35)$$

where $\Xi = \mathbb{S}^3 \times \mathbb{R}^3 \times \mathbb{R}^3 \times \mathbb{R}^3 \times \mathbb{S}^3 \subseteq \mathbb{R}^{17}$ and the compact set

$$\mathscr{A}_\circ := \big\{ \boldsymbol{\xi} \in \Xi \mid \mathbf{q}_\Delta = \mathbf{q}_I, \boldsymbol{\omega}_\Delta = \mathbf{0}, \mathbf{z} = \mathbf{0}, \mathbf{e} = \mathbf{0}, $$
$$\mathbf{R}(\mathbf{q})\mathbf{d}_* = \mathbf{e}_3\|\mathbf{d}_*\| \big\}, \quad (36)$$

which clearly characterizes the requirement that the desired position is asymptotically reached ($\mathbf{e} = \mathbf{0}$), with some constant orientation ensuring that the zero-moment direction $\mathbf{d}_*$ is correctly aligned with the steady-state action $mg\mathbf{e}_3$, necessary for counteracting the gravity force. Note that set $\mathscr{A}_\circ$ is compact because it is the product of compact sets.

Thanks to the a hierarchical (or cascade-like) structure of the error dynamics, we can prove the following theorem using a Lyapunov-based approach and the suitable reduction theorems for the stability of nested sets presented in El-Hawwary and Maggiore (2013). The complete proof is here omitted due to space constraints.

Theorem 1. Consider the closed-loop system represented in Figure 1 between plant (11)–(13) and the controller presented in Section 4.2. The compact set $\mathscr{A}_\circ$ in (36) is asymptotically stable for the corresponding dynamics.

5. SIMULATION RESULTS

The effectiveness of the proposed controller for solving Problem 1 is here validated by numerical simulations carried out on a hexarotor characterized by six tilted propellers.

To exhaustively describe the evaluated platform, let us introduce the frames $\mathscr{F}_{P_1}, \ldots, \mathscr{F}_{P_6}$, with $\mathscr{F}_{P_i} = \{O_{P_i}, (\mathbf{x}_{P_i}, \mathbf{y}_{P_i}, \mathbf{z}_{P_i})\}$. The origin O_{P_i} coincides with the CoM of the i-th propeller, $\mathbf{x}_{P_i}$ and $\mathbf{y}_{P_i}$ identify its spinning plane, while $\mathbf{z}_{P_i}$ coincides with its spinning axis. In our case study, $O_{P_1} \ldots O_{P_6}$ lie on the $\mathbf{x}_B\mathbf{y}_B$ plane where they are equally spaced along a circle. Hence, for $i \in \{1, \ldots, n\}$, the position $\mathbf{p}_i \in \mathbb{R}^3$ of O_{P_i} in $\mathscr{F}_B$ is set as

$$\mathbf{p}_i = \mathbf{q}(\lambda_i, \mathbf{e}_3) \otimes [0 \ L \ 0]^\top \otimes \mathbf{q}(\lambda_i, \mathbf{e}_3)^{-1} \qquad (37)$$

where $\mathbf{q}(\lambda_i, \mathbf{e}_3)$ is the unit quaternion associated to the rotation by $\lambda_i = (i-1)\pi/3$ about $\mathbf{e}_3$ according to (3), and $L > 0$ is the distance between O_{P_i} and O_B. In addition, we assume that the

orientation of each $\mathscr{F}_{P_i}$ w.r.t. $\mathscr{F}_B$ can be represented by the unit quaternion $\mathbf{q}_i \in \mathbb{S}^3$ such that

$$\mathbf{q}_i = \mathbf{q}(\lambda_i, \mathbf{e}_3) \otimes \mathbf{q}(\beta_i, \mathbf{e}_2) \otimes \mathbf{q}(\alpha_i, \mathbf{e}_1) \qquad (38)$$

where $\mathbf{q}(\beta_i, \mathbf{e}_2)$ and $\mathbf{q}(\alpha_i, \mathbf{e}_1)$ agree with the representation (3). The tilt angles $\alpha_i, \beta_i \in [-\pi, \pi]$ uniquely define the direction of $\mathbf{z}_{P_i}$ in $\mathscr{F}_B$. Indeed, the frame $\mathscr{F}_{P_i}$ is obtained from $\mathscr{F}_B$ by first rotating by α_i about $\mathbf{x}_B$ and then by β_i around $\mathbf{y}'_B$. These angles are chosen so that $\alpha_i = -\alpha_{i+1}$ and $\alpha_i \neq \alpha_j$ for $i,j = 1,3,5$, while $\beta_i = \beta$ for $i = 1, \ldots, 6$.

This configuration satisfies Assumption 1. In detail, matrix $\mathbf{F}_1$ is full-rank, and $\mathbf{K}$ can be chosen as the product between an orthogonal basis of the null space of $\mathbf{F}_1$ and its transpose, which is not in the null space of $\mathbf{F}_2$.

In this framework, the control task is to steer (and to keep) the hexarotor to a locally stable equilibrium position $\mathbf{p}_r = [0.2 \ 0.5 \ 0.8]^\top$ starting from the initial position which is fixed at the origin of the inertial frame, i.e., $\mathbf{p}_0 = [0 \ 0 \ 0]^\top$. In addition, the stabilization of the platform attitude is required. To this aim, the gains of the controller are set as follows: $k_{pp} = 4$, $k_{pd} = 8$, $k_{ap} = 2$, $k_{ad} = 4$, $k_z = 15$, which induce desirable transients on the equivalent PD-like error dynamics.

The simulation results are depicted in Figure 2. In the first and second plot, we show the position and the orientation of the hexarotor, respectively. The use of the roll-pitch-yaw angles (ϕ, θ, ψ) to represent the attitude is to give a better insight of the vehicle behavior; however, the internal computations are all done with unit quaternions. The hexarotor smoothly achieves the reference position in roughly 10s. After this transient, the position error $\mathbf{e}_p$ (third plot) converges to zero. On the other hand, the orientation $\mathbf{q} \to (\phi, \theta, \psi)$ of the vehicle converges to the desired one $\mathbf{q}_d \to (\phi_d, \theta_d, \psi_d)$ with a comparable transient period but a very small initial mismatch that it is barely seen in the second plot while its entity is clearly observable in the fourth plot that reports the trend of the roll-pitch-yaw angles $(\phi_\Delta, \theta_\Delta, \psi_\Delta)$ associated to the quaternion $\mathbf{q}_\Delta$. For the sake of completeness, the last plot in Figure 2 illustrates the control inputs provided to each propeller: at the steady state all the spinning rates are included in $[58, 68]$ Hz that represents a feasible range of values from the practical point of view.

To prove the robustness of the controller, the same control goal is achieved introducing some non idealities in the model: delays and Gaussian noise are added to approximate the performance of a real system. The plots in Figure 3 prove that the errors still converge to zero and the control inputs belong to a feasible range although their evolution is corrupted by noise. This behavior is expected in light of robustness results of asymptotic stability of compact attractors (Goebel et al., 2012, Chap.7).

6. CONCLUSIONS

In this work we address the control task of stabilizing a multi-rotor platform to a given reference position with an arbitrary but constant orientation. No restrictive assumption is made on the vehicle structure (whose propellers are arbitrary in number and spinning axis mutual orientation), however the proposed solution is based on some algebraic properties for the control matrices $\mathbf{F}_1$ and $\mathbf{F}_2$. We design a state feedback nonlinear controller mainly based upon the existence of a preferential direction in the feasible force space, along which the control force

and the control moment are decoupled. Numerical simulation results show the effectiveness of the proposed control law.

As future works, we aim at extending the control goal to both the tracking of a dynamic position trajectory and the stabilization on a given reference orientation. For both these cases, some preliminary results are already available but here omitted for lack of space.

REFERENCES

Argentim, L.M., Rezende, W.C., Santos, P.E., and Aguiar, R.A. (2013). PID, LQR and LQR-PID on a quadcopter platform. In *Informatics, Electronics Vision (ICIEV), 2013 International Conference on*, 1–6.

Bouabdallah, S. and Siegwart, R. (2005). Backstepping and sliding-mode techniques applied to an indoor micro quadrotor. In *Proceedings of the 2005 IEEE International Conference on Robotics and Automation*, 2247–2252.

Carrillo, L.G., Dzul, A., and Lozano, R. (2012). Hovering quad-rotor control: A comparison of nonlinear controllers using visual feedback. *IEEE Transactions on Aerospace and Electronic Systems*, 48(4), 3159–3170.

Choi, Y.C. and Ahn, H.S. (2015). Nonlinear control of quadrotor for point tracking: Actual implementation and experimental tests. *IEEE/ASME transactions on mechatronics*, 20(3), 1179–1192.

Diebel, J. (2006). Representing attitude: Euler angles, unit quaternions, and rotation vectors. *Matrix*, 58(15-16), 1–35.

El-Hawwary, M. and Maggiore, M. (2013). Reduction theorems for stability of closed sets with application to backstepping control design. *Automatica*, 49(1), 214–222.

Erginer, B. and Altug, E. (2007). Modeling and PD control of a quadrotor VTOL vehicle. In *2007 IEEE Intelligent Vehicles Symposium*, 894–899.

Goebel, R., Sanfelice, R.G., and Teel, A.R. (2012). *Hybrid Dynamical Systems: modeling, stability, and robustness.* Princeton University Press.

Hua, M.D., Hamel, T., Morin, P., and Samson, C. (2013). Introduction to feedback control of underactuated VTOL vehicles: A review of basic control design ideas and principles. *IEEE Control Systems Magazine*, 33(1), 61–75.

Lee, D., Jin Kim, H., and Sastry, S. (2009). Feedback linearization vs. adaptive sliding mode control for a quadrotor helicopter. *International Journal of Control, Automation and Systems*, 7(3), 419–428.

Lee, T., Leoky, M., and McClamroch, N.H. (2010). Geometric tracking control of a quadrotor UAV on SE(3). In *49th IEEE Conf. on Decision and Control*, 5420–5425. Atlanta, GA.

Mahony, R., Kumar, V., and Corke, P. (2012). Multirotor aerial vehicles: Modeling, estimation, and control of quadrotor. *IEEE Robotics Automation Magazine*, 19(3), 20–32.

Michieletto, G., Ryll, M., and Franchi, A. (2017). Control of statically hoverable multi-rotor aerial vehicles and application to rotor-failure robustness for hexarotors. In *2017 IEEE Int. Conf. on Robotics and Automation*. Singapore.

Mistler, V., Benallegue, A., and M'Sirdi, N.K. (2001). Exact linearization and noninteracting control of a 4 rotors helicopter via dynamic feedback. In *10th IEEE Int. Symp. on Robots and Human Interactive Communications*, 586–593. Bordeaux, Paris, France.